Available online at www.sciencedirect.com
ScienceDirect
Trans. Nonferrous Met. Soc. China 25(2015) 2725−2733
Transactions of Nonferrous Metals Society of China
www.tnmsc.cn

Surface species of chalcopyrite during bioleaching by moderately thermophilic bacteria

Hong-bo ZHAO[1,2], Jun WANG[1,2], Wen-qing QIN[1,2], Xi-hua ZHENG[1,2], Lang TAO[1,2], Xiao-wen GAN[1,2], Guan-zhou QIU[1,2]

1. School of Minerals Processing and Bioengineering, Central South University, Changsha 410083, China;
2. Key Laboratory of Bio-hydrometallurgy of Ministry of Education, Central South University, Changsha 410083, China

Received 29 December 2014; accepted 3 April 2015

Abstract: X-ray diffraction (XRD) and X-ray photoelectron spectroscopy (XPS) analyses were carried out to investigate the surface species and interfacial reactions during bioleaching of chalcopyrite by different strains of moderately thermophilic bacteria (45 °C). Results show that monosulfide (CuS), disulfide (S_2^{2-}), polysulfide (S_n^{2-}), elemental sulfur (S^0) and sulfate (SO_4^{2-}) are the main intermediate species on the surface of chalcopyrite during bioleaching by *A. caldus*, *S. thermosulfidooxidans* and *L. ferriphilum*. The low kinetics of dissolution of chalcopyrite in *A. caldus* can be mainly attributed to the incomplete dissolution of chalcopyrite and the passivation layer of polysulfide. Polysulfide and jarosite should be mainly responsible for the passivation of chalcopyrite in bioleaching by *L. ferriphilum* or *S. thermosulfidooxidans*. However, elemental sulfur should not be the main composition of passivation layer of chalcopyrite during bioleaching.

Key words: chalcopyrite; surface species; bioleaching; passivation; moderately thermophilic bacteria

1 Introduction

As a promising technology in processing low grade ores, bio-hydrometallurgy has been successfully applied for the recovery of metals such as copper, nickel, zinc, and refractory gold [1,2]. Chalcopyrite ($CuFeS_2$) is the most abundant and widespread copper-bearing mineral, accounting for approximately 70% of the copper resources [3,4]. However, it is still difficult to be effectively extracted by bioleaching mainly due to the low kinetics [5].

It has been generally accepted that the main cause of low leaching efficiency of chalcopyrite in bioleaching is the formation of passivation layer, which can inhibit the further dissolution of chalcopyrite [6−9]. Many researchers have focused on interpreting the dissolution process and the compositions of passivation layer, and different conclusions were proposed. Among the proposed conclusions, elemental sulfur, metal-deficient polysulfide and iron-hydroxyl compounds mainly consisting of jarosite were considered as the main compositions of passivation layer, but the specific compositions of passivation layer and the dissolution pathway are still being debated [8,10]. This can be mainly attributed to the differences of bioleaching systems, especially the bacteria used in bioleaching.

Three main types of microorganisms were classified according to their optimum growth temperature, including mesophiles, moderately thermophilic bacteria and extreme thermophilic bacteria [6,7]. Chalcopyrite can be easily passivated under the temperature less than 35 °C, and the extreme thermophilic bacteria are sensitive to high shear force caused by high pulp density as the absence of cytoderm, which restrict the further industrial application [2,11]. Moderately thermophilic bacteria are suitable to grow in heap and tank bioleaching as the relatively high temperature in heap and bioreactor, and they have a more extensive application prospect compared with the other two types

Foundation item: Projects (51374248, 51320105006) supported by the National Natural Science Foundation of China; Project (NCET-13-0595) supported by the Program for New Century Excellent Talents in University, China; Project (2014T70692) supported by China Postdoctoral Science Foundation

Corresponding author: Jun WANG; Tel: +86-731-88876557; E-mail: wjwq2000@126.com

DOI: 10.1016/S1003-6326(15)63897-3

of microorganisms [2,12].

Additionally, the intermediate species are usually with trace amount, and the passivation layer is usually too thin to be directly detected by the normal X-ray diffraction method [13]. X-ray photoelectron spectroscopy (XPS) has been widely used to characterize the surface layers, and it can provide reliable data on the chemical states of the surface species [13−15].

Therefore, in the present work, the compositions of formed product layers on chalcopyrite surface in bioleaching by moderately thermophilic bacteria were investigated mainly by X-ray photoelectron spectroscopy (XPS) to interpret the electrochemical dissolution process and the mechanisms of passivation.

2 Experimental

2.1 Materials

Chalcopyrite sample was obtained from geological museum of Guangxi Province of China. X-ray diffraction analysis (XRD) (Fig. 1) showed that it was of high purity. The chemical analysis showed that the chalcopyrite sample contained 34.46% Cu, 31.53% Fe, and 33.12% S (mass fraction), respectively. Ore samples were ground and sieved to less than 0.074 mm before being used for leaching experiments. All chemicals used were of analytical purity in this work.

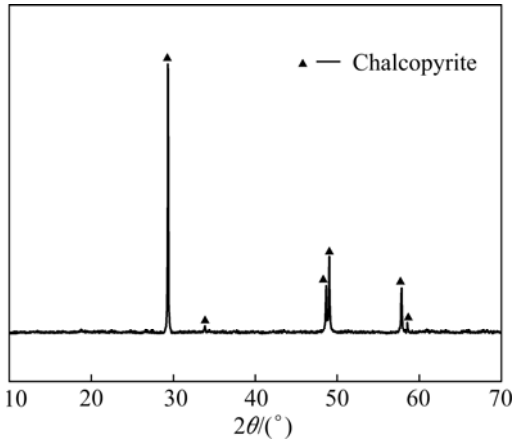

Fig. 1 XRD pattern of untreated chalcopyrite

2.2 Microorganisms and culture media

Moderately thermophilic bacteria, including *Acidithiobacillus caldus* (*A. caldus*), *Sulfobacillus thermosulfidooxidans* (*S. thermosulfidooxidans*) and *Leptospirillum ferriphilum* (*L. ferriphilum*), were obtained from the Key Laboratory of Bio-hydrometallurgy of Ministry of Education, Central South University, China. Bacteria were cultured in 250 mL shake flasks in an orbital incubator with a stirring speed of 170 r/min at a temperature of 45 °C. The basic culture medium was composed of the following compositions: $(NH_4)_2SO_4$ (3.0 g/L), $MgSO_4·7H_2O$ (0.5 g/L), K_2HPO_4 (0.5 g/L), KCl (0.1 g/L), $Ca(NO_3)_2$ (0.01 g/L). *L. ferriphilum* and *A. caldus* were sub-cultured into basal salts medium supplemented with 44.7 g/L ferrous sulphate ($FeSO_4·7H_2O$) and 10 g/L sulfur as energy sources, respectively. *S. thermosulfidooxidans* were sub-cultured into basal salts medium supplemented with 44.7 g/L ferrous sulphate ($FeSO_4·7H_2O$) and 10 g/L sulfur as energy sources. The resulting culture was used as inoculums for the bioleaching experiments.

2.3 Bioleaching experiments

10 mL of cell solution was inoculated into a 250 mL shake flask containing 90 mL of sterilized culture medium and 2 g of minerals. The initial cell concentration of bacteria was higher than 1.0×10^7 cells/mL. The shake flasks were placed into an orbital shaker at 170 r/min and 45 °C, pH value was adjusted to 1.7 by sulfuric acid regularly, and water lost by evaporation was supplemented periodically by adding deionized water. Copper concentrations were determined by inductively coupled plasma-atomic emission spectrometer (ICP-AES) (America Baird Co. PS−6). The pH values were measured with a pH meter (PHSJ−4A) and the redox potentials of leaching solution were measured by a Pt electrode with reference to a Ag/AgCl electrode (3.0 mol/L KCl) (BPP−922). The mineralogical compositions of solid samples were examined by X-ray diffraction (XRD) (DX−2700).

2.4 X-ray photoelectron spectroscopy (XPS)

The samples in different stages of bioleaching (7, 15, 22 d) were filtered and rinsed with deionized water three times, then transferred to vacuum drying oven (DZF−6050) to dry before X-ray photoelectron experiment (XPS) measurements.

X-ray photoelectron experiment (XPS) measurements were carried out on the model of ESCALAB 250Xi. Spectra were recorded at constant pass energy of 20 eV and energy step size of 0.1 eV, with Al K_α X-ray as the source. Binding energy calibration was based on C 1s at 284.6 eV. Thermo Avantage 5.52 software was used for fitting the XPS peaks. The Shirley method was chosen for obtaining the background of spectra, and the S 2p spectra were fitted by Gaussian−Lorentzian line (SGL) function.

3 Results and discussion

3.1 Bioleaching behaviors

Figure 2 shows that redox potential of bioleaching by *A. caldus* maintained at a low and steady value throughout the bioleaching process, during which the copper extraction continued to increase slowly and

steadily. Redox potential of bioleaching by *S. thermosulfidooxidans* started to increase sharply from the 5th day, and reached a high value of about 600 mV on the 10th day. Correspondingly, the copper extraction kept increasing significantly in the first 10 d, and then stopped. For bioleaching of chalcopyrite by *L. ferriphilum*, redox potential started to increase sharply from the 10th day, and arrived at the value of more than 600 mV on the 15th day. Accordingly, the copper extraction continued increasing significantly in the first 15 d, and then stagnated. This distinctly revealed that kinetics of bioleaching by *A. caldus* was low, and chalcopyrite was easy to be passivated in bioleaching by *S. thermosulfidooxidans* and *L. ferriphilum*.

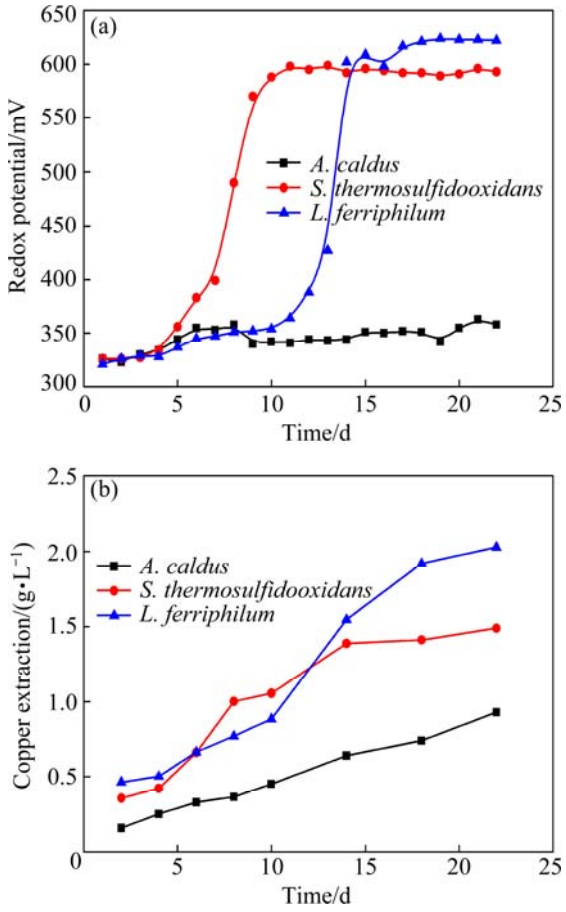

Fig. 2 Bioleaching of chalcopyrite by moderately thermophilic bacteria: (a) Redox potential; (b) Copper extraction

Redox potential was mainly determined by the concentration ratio of ferric to ferrous ions (Fe^{3+}/Fe^{2+}), so the sharp increase of redox potential can be mainly attributed to the oxidation of ferrous to ferric ions by *S. thermosulfidooxidans* and *L. ferriphilum*. In addition, redox potential was an important, even a determining factor in bioleaching of chalcopyrite. Many researchers have proposed that dissolution of chalcopyrite can be accelerated by controlling redox potential at a relatively low value, and extremely high redox potentials can easily cause the passivation of chalcopyrite, thus inhibiting its further dissolution [16−19]. To further investigate the causes of low kinetics and passivation of chalcopyrite in bioleaching, XRD and XPS were used to analyze the intermediate species on chalcopyrite surface in different stages of bioleaching.

Figure 3 presents the mineralogical compositions of samples after bioleaching by *A. caldus*, *S. thermosulfidooxidans* and *L. ferriphilum* for 7, 15, and 22 d, respectively. It can be found that elemental sulfur formed

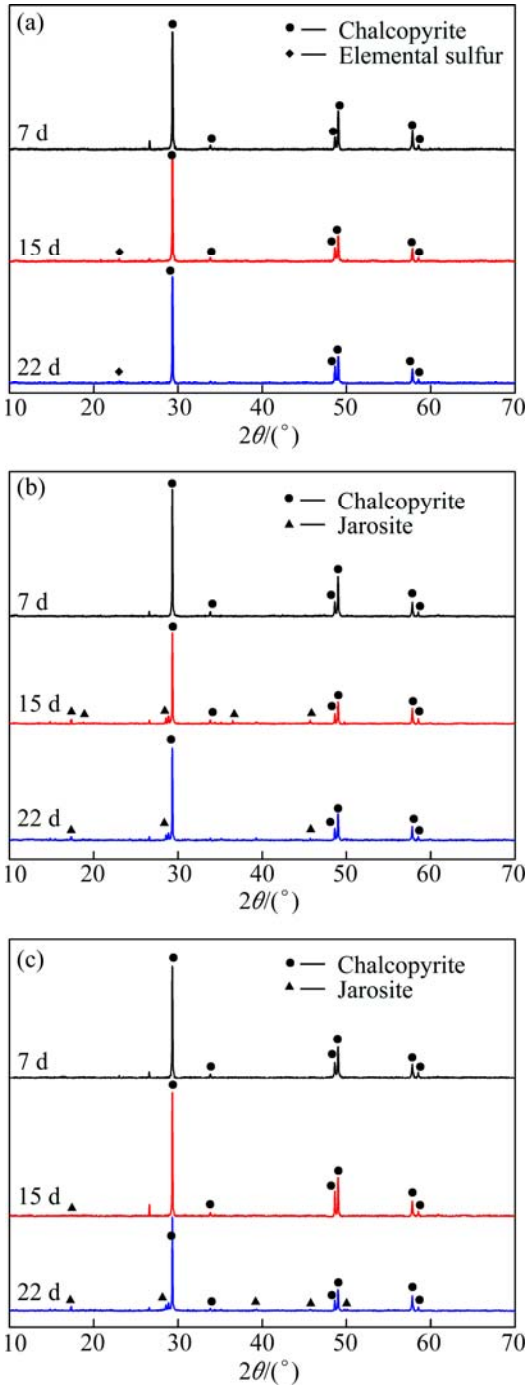

Fig. 3 Mineralogical compositions of samples leached by different strains of bacteria: (a) *A. caldus*; (b) *S. thermosulfidooxidans*; (c) *L. ferriphilum*

at the later stage of bioleaching by *A. caldus*, while significant amount of jarosite formed at the later stage of bioleaching by *S. thermosulfidooxidans* and by *L. ferriphilum*.

3.2 X-ray photoelectron spectroscopy (XPS) analysis

XPS can provide reliable data to determine the trace amounts of intermediate species during the bioleaching process. Hence, the samples leached for 7, 15 and 22 d were analyzed by XPS, and the obtained survey XPS spectra are shown in Fig. 4. The Cu 2p, Cu LMM and S 2p peaks were further analyzed. For convenience, the stage of the first 7 d was described as the initial stage, 7−15 d was defined as the middle stage, and 15−22 d was represented by the later stage.

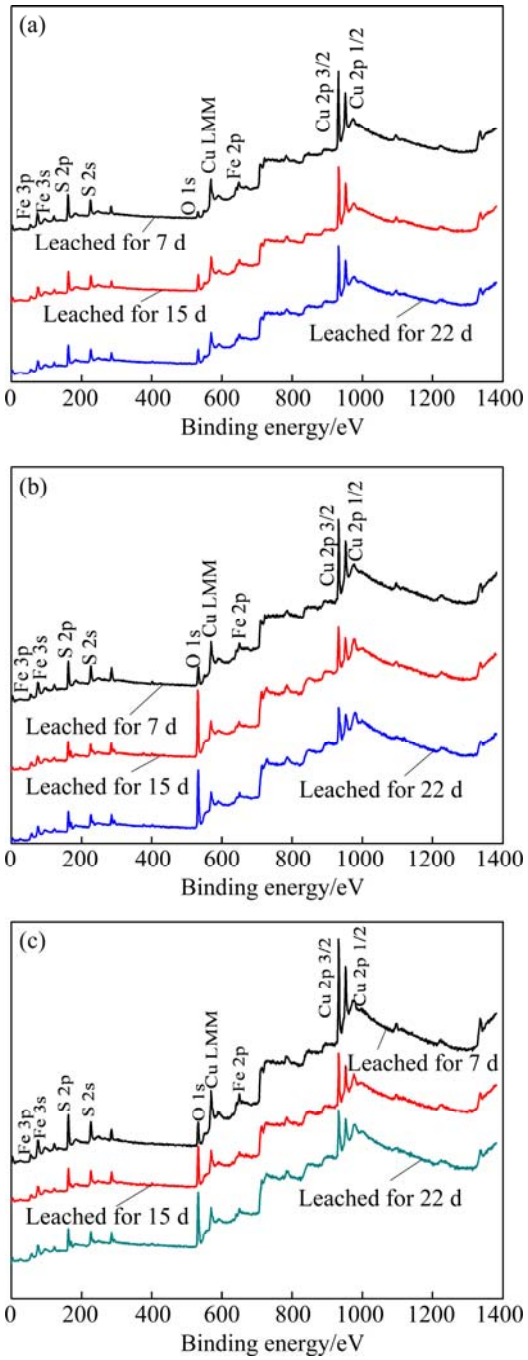

Fig. 4 Survey (full range) XPS spectra of samples leached by different strains of bacteria: (a) *A. caldus*; (b) *S. thermosulfidooxidans*; (c) *L. ferriphilum*

Figure 5(a) shows the Cu 2p peaks of samples after bioleaching by *A. caldus* for 7, 15, and 22 d, respectively. The two peaks of Cu $2p_{3/2}$ and Cu $2p_{1/2}$ were centered at 932.1 and 952.0 eV, respectively. Both of the Cu $2p_{3/2}$ and Cu $2p_{1/2}$ peaks were centered at lower binding energy than that of chalcopyrite (932.4, 952.1 eV) [20]. It has been well demonstrated that Cu $2p_{3/2}$ peak with binding energy (933.0−933.8 eV) and the presence of a shake-up peak (939−944 eV) are the two major XPS characteristics of cupric species, while a lower binding energy of Cu $2p_{3/2}$ peak (931.8−933.1 eV) and the absence of the shake-up peak are the characteristics of cuprous species, including Cu_2O (932.4 eV), CuS (932.0−932.4 eV) and Cu_2S (932.9 eV) [20−24]. By comparison, it can be speculated that CuS may be the possible cuprous species. Figure 5(b) shows that the Cu LMM peaks of the three samples were centered at 568.7 eV. The corresponding values of Cu LMM peaks of Cu_2O, Cu_2S and CuS were reported at 569.7, 569.5 and 568.5 eV, respectively [23,24]. Therefore, CuS can be the most plausible cuprous species during bioleaching

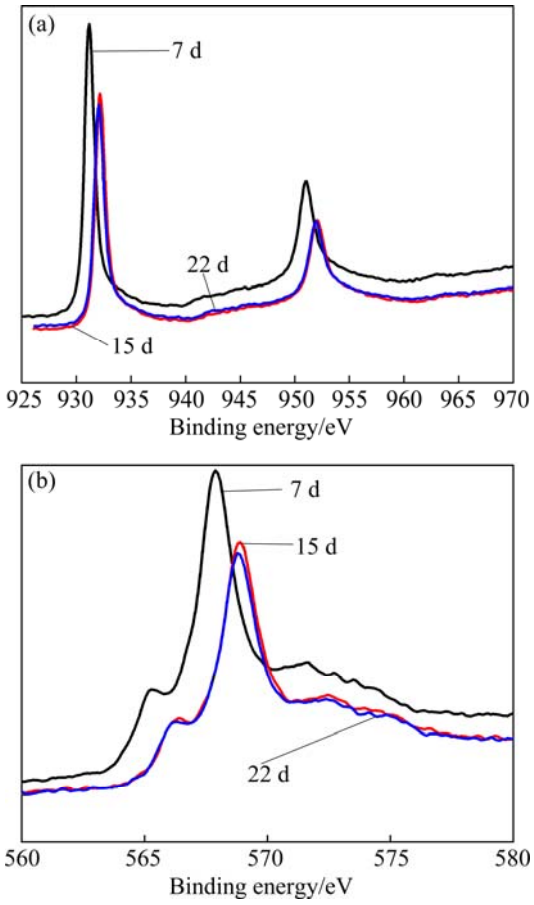

Fig. 5 XPS spectra of Cu peaks of chalcopyrite leached by *A. caldus* for different time: (a) Cu 2p peak; (b) Cu LMM peak

of chalcopyrite by *A. caldus*.

Figure 6(a) presents the Cu 2p peaks of samples after bioleaching by *S. thermosulfidooxidans* for 7, 15, and 22 d, respectively. The Cu $2p_{3/2}$ peaks of the three samples were centered at 931.8 eV, which was approximately equal to the value of Cu $2p_{3/2}$ peak of CuS (932.0−932.4 eV) [20]. In addition, Fig. 6(b) shows that the Cu LMM peaks were centered at 568.5−568.7 eV, which was in consistent with that of Cu LMM peak of CuS (568.5 eV) [24]. Hence, CuS can be the most possible cuprous species during bioleaching of chalcopyrite by *S. thermosulfidooxidans*.

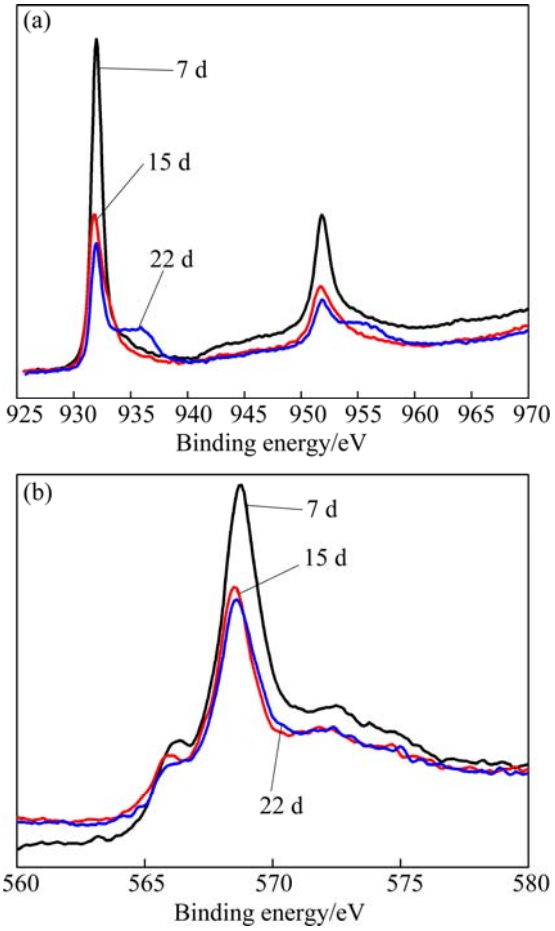

Fig. 6 XPS spectra of Cu peaks of chalcopyrite leached by *S. thermosulfidooxidans* for different time: (a) Cu 2p peak; (b) Cu LMM peak

Figure 7(a) compares the Cu 2p spectra of samples after bioleaching by *L. ferriphilum* for different time. The Cu $2p_{3/2}$ peaks of the three samples were centered at 932.0 eV, which agreed well with that of Cu $2p_{3/2}$ peak of CuS (932.0−932.4 eV) [20]. Figure 7(b) shows that the Cu LMM peaks of the three samples were centered at 568.5−568.7 eV, which was almost equal to that of Cu LMM peak of CuS (568.5 eV) [24]. Therefore, CuS can be the most receivable cuprous species during bioleaching of chalcopyrite by *L. ferriphilum*.

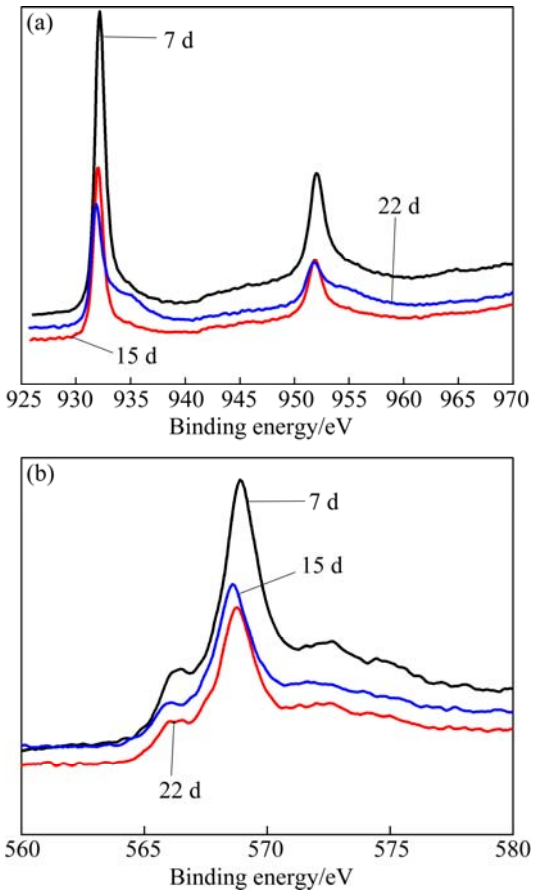

Fig. 7 XPS spectra of Cu peaks of chalcopyrite leached by *L. ferriphilum* for different time: (a) Cu 2p peak; (b) Cu LMM peak

According to the above results, it can be concluded that CuS is the main cuprous species on the surface of chalcopyrite during bioleaching by *A. caldus*, *S. thermosulfidooxidans* and *L. ferriphilum*. Similarly, in some other researches, the formation of CuS on the surface of chalcopyrite in leaching process and electrochemical measurements has been detected [9,13,25−28].

Sulfur species can be mainly classified as monosulfide (S^{2-}, binding energy: 161.1−161.8 eV; FWHM: 0.5−0.7 eV), disulfide (S_2^{2-}, binding energy: 162.3−162.4 eV; FWHM: 0.5−0.7 eV), polysulfide (S_n^{2-}, binding energy: 163.0−163.9 eV; FWHM: 1.1−1.3 eV), elemental sulfur (S^0, binding energy: 163.05−164.7 eV; FWHM: 0.7−1.7), sulfite (SO_3^{2-}, binding energy: 166.4−166.5 eV), thiosulfate (S_2O_3, binding energy: 161.7−163.2 eV; 167.4−167.8 eV) and sulfate (SO_4^{2-}, binding energy: 168.0−169.0; FWHM: 0.9), respectively [8,29−32].

Figure 8 shows the XPS spectra of S 2p peaks of samples leached by *A. caldus* for 7, 15 and 22 d, respectively. Monosulfide, disulfide, polysulfide and elemental sulfur were the main sulfur species on the surface of chalcopyrite during bioleaching by *A. caldus*.

Figure 9 shows the percentages of sulfur species on the surface of chalcopyrite leached by *A. caldus* for different time. Monosulfide and polysulfide were the most abundant sulfur species throughout the bioleaching process. The percentage of polysulfide was kept at more than 20% throughout the bioleaching process. However, the percentage of elemental sulfur was always less than 6% during the bioleaching process. Therefore, it can be inferred that the formed polysulfide should be the main composition of passivation layer in bioleaching of chalcopyrite by *A. caldus*.

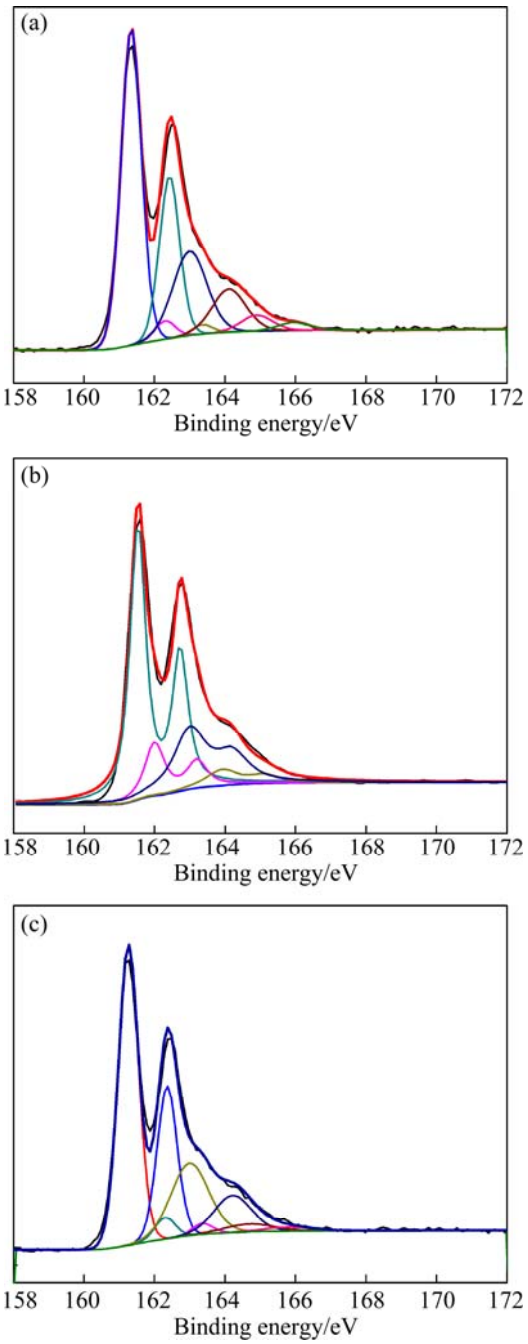

Fig. 8 XPS spectra of S 2p peaks of chalcopyrite leached by *A. caldus* for different time: (a) 7 d; (b) 15 d; (c) 22 d

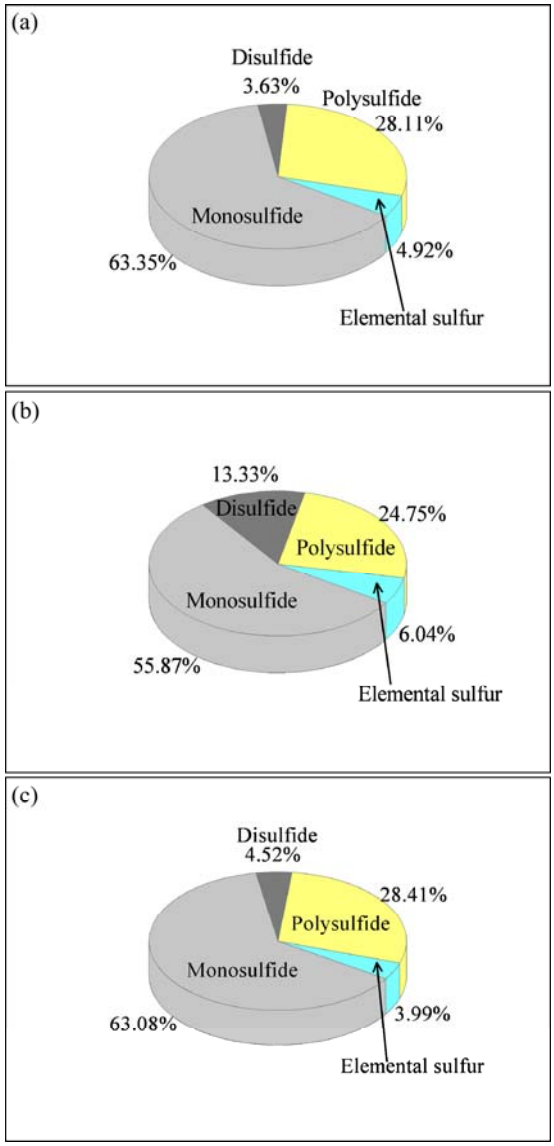

Fig. 9 Percentages sulfur species on surface of chalcopyrite leached by *A. caldus* for different time: (a) 7 d; (b) 15 d; (c) 22 d

Figure 10 provides the XPS spectra of S 2p peaks of samples leached by *S. thermosulfidooxidans* for 7, 15 and 22 d, respectively. By fitting the peaks, monosulfide, disulfide and polysulfide can be considered as the main sulfur species on the surface of chalcopyrite leached by *S. thermosulfidooxidans* for 7 d. Except for monosulfide, disulfide and polysulfide, sulfate can be detected on the 15th and 22nd days. The formed sulfate mainly consisted of jarosite according to the analytical results of XRD analysis. The percentages of sulfur species on the surface of chalcopyrite leached by *S. thermosulfidooxidans* for different time are shown in Fig.11, which revealed that the percentage of polysulfide remained at more than 20% throughout the bioleaching process, and a high percentage of about 20% of sulfate was formed from the 15th day of bioleaching. However, the percentage of

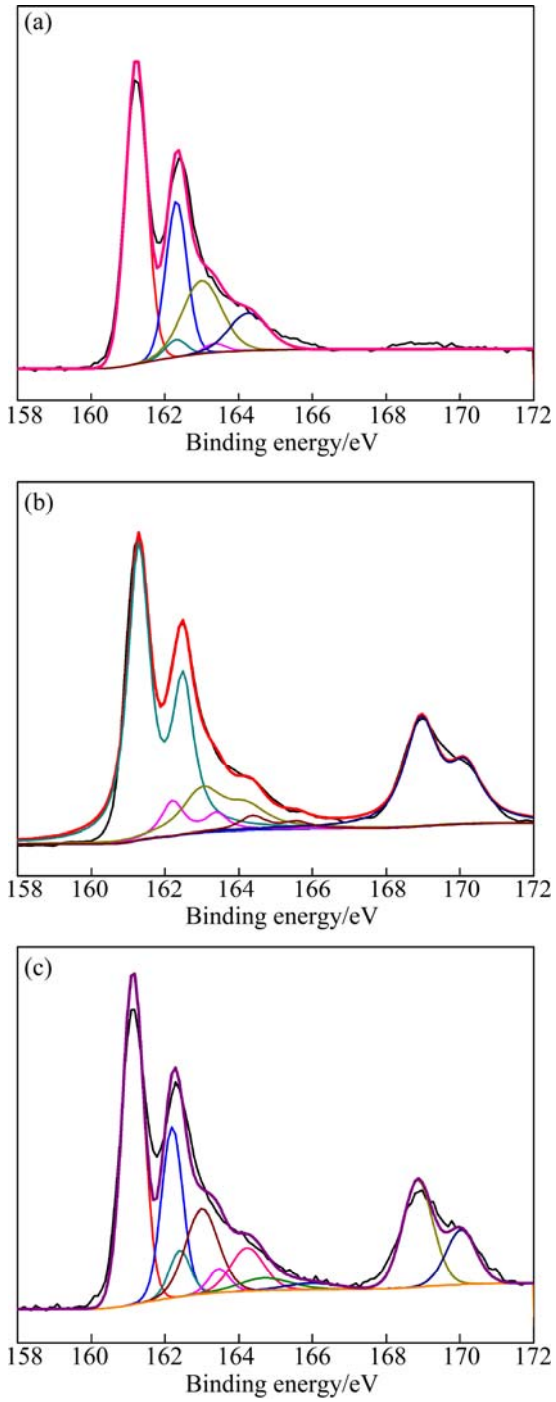

Fig. 10 XPS spectra of S 2p peaks of chalcopyrite leached by *S. thermosulfidooxidans* for different time: (a) 7 d; (b) 15 d; (c) 22 d

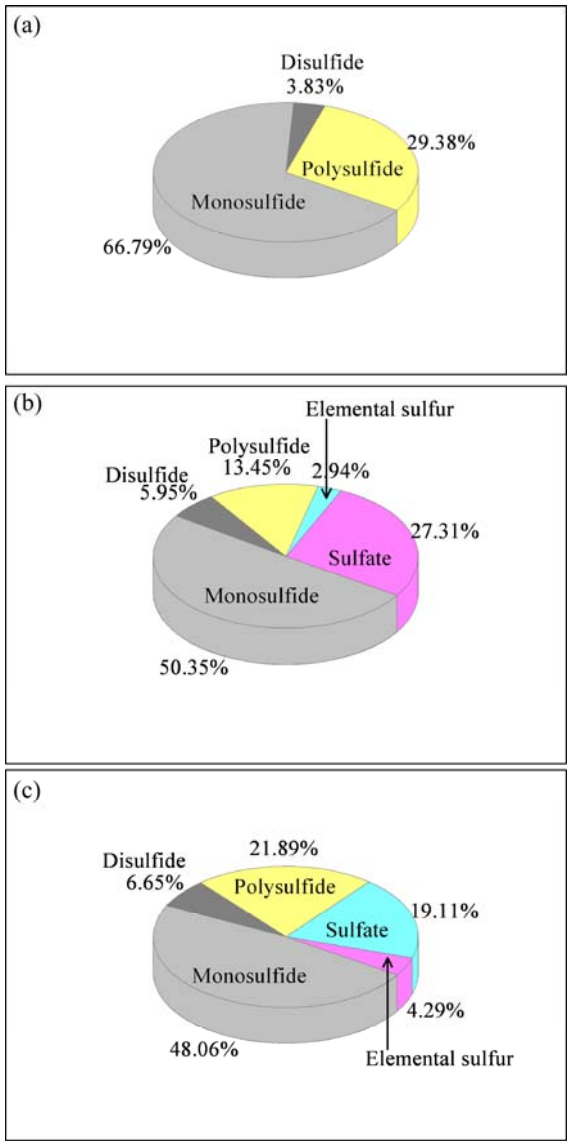

Fig. 11 Percentages of sulfur species on surface of chalcopyrite leached by *S. thermosulfidooxidans* for different time: (a) 7 d; (b) 15 d; (c) 22 d

elemental sulfur was less than 5% throughout the bioleaching process. Therefore, polysulfide and sulfate should mainly be responsible for the passivation of chalcopyrite during bioleaching by *S. thermosulfidooxidans*.

Figure 12 shows the XPS spectra of S 2p peaks of samples leached by *L. ferriphilum* for 7, 15 and 22 d, respectively. Sulfur species of monosulfide, disulfide and polysulfide can be detected on the surface of chalcopyrite leached for 7 d. Monosulfide, disulfide, polysulfide, elemental sulfur and sulfate mainly consisting of jarosite were the main sulfur species on the surface of chalcopyrite leached for 15 and 22 d. Figure 13 provides the compositions of sulfur species on the surface of chalcopyrite in different stages of bioleaching. It can be found that polysulfide kept at a relatively stable percentage of more than 18%, and a significant amount of sulfate species was formed from the middle stage of bioleaching. Moreover, the percentage of elemental sulfur was less than 5% during the whole bioleaching process. Therefore, the formed polysulfide and jarosite can be the main compositions of passivation layer in bioleaching of chalcopyrite by *L. ferriphilum*.

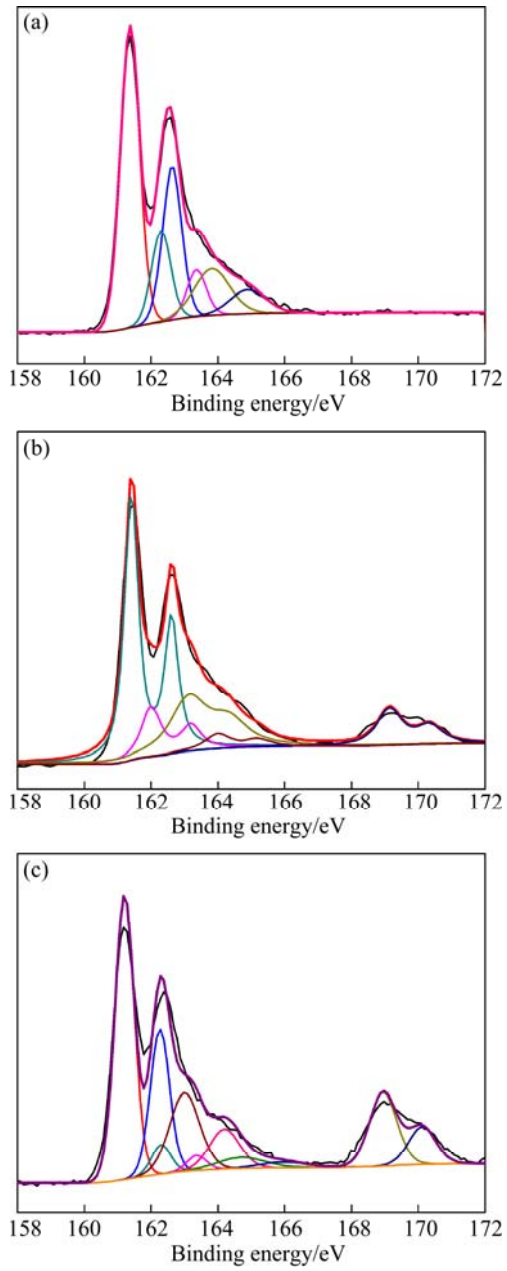

Fig. 12 XPS spectra of S 2p peaks of chalcopyrite leached by *L. ferriphilum* for different time: (a) 7 d; (b) 15 d; (c) 22 d

4 Conclusions

1) Monosulfide (CuS), disulfide (S_2^{2-}), polysulfide (S_n^{2-}), elemental sulfur (S^0) and sulfate (SO_4^{2-}) are the main intermediate species on the surface of chalcopyrite during bioleaching by *A. caldus*, *S. thermosulfidooxidans* and *L. ferriphilum*.

2) For bioleaching of chalcopyrite by *A. caldus*, the selective dissolution of iron elements causes the formation of metal-deficient polysulfide, which should be the main composition of the passivation layer. Polysulfide and jarosite can be mainly responsible for the passivation of chalcopyrite in bioleaching by *L. ferriphilum* or *S. thermosulfidooxidans*. Moreover, elemental sulfur should not be the main cause of passivation of chalcopyrite during bioleaching.

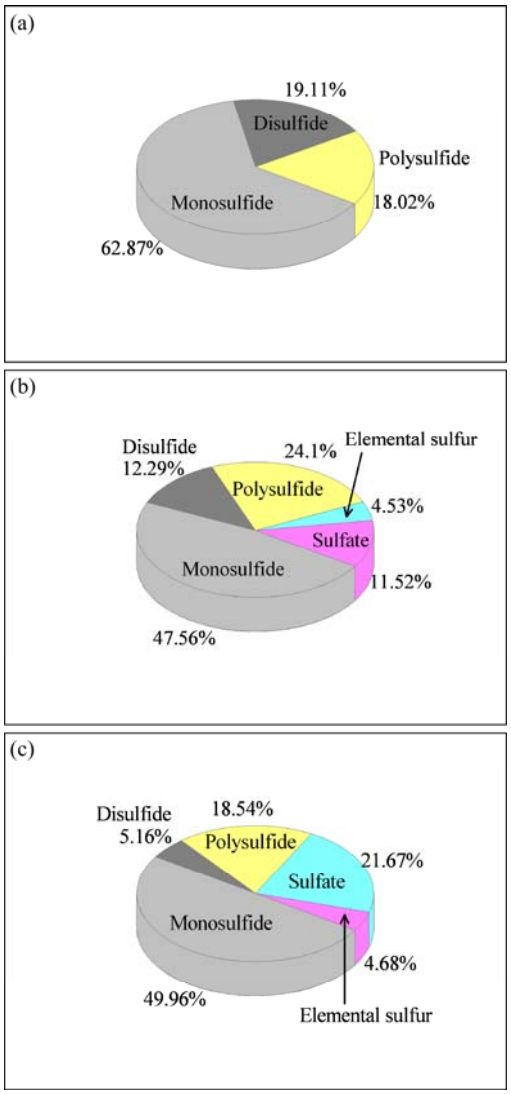

Fig. 13 Percentages of sulfur species on surface of chalcopyrite leached by *L. ferriphilum* for different time: (a) 7 d; (b) 15 d; (c) 22 d

References

[1] VERA M, SCHIPPERS A, SAND W. Progress in bioleaching: Fundamentals and mechanisms of bacterial metal sulfide oxidation. Part A [J]. Applied Microbiology and Biotechnology, 2013, 97(17): 7529−7541.

[2] WANG Jun, QIN Wen-qing, ZHANG Yan-sheng, YANG Cong-ren, ZHANG Jian-wen, NAI Shao-shi, SHANG He, QIU Guan-zhou. Bacterial leaching of chalcopyrite and bornite with native bioleaching microorganism [J]. Transactions of Nonferrous Metals Society of China, 2008, 18(6): 1468−1472.

[3] HABASHI F. Chalcopyrite. Its chemistry and metallurgy [M]. Quebec Canada: Laval University, 1978.

[4] CORDOBA E M, MUNOZ J A, BLAZQUEZ M L, GONZALEZ F, BALLESTER A. Leaching of chalcopyrite with ferric ion. Part I: General aspects [J]. Hydrometallurgy, 2008, 93(3): 81−87.

[5] WATLING H. The bioleaching of sulphide minerals with emphasis on copper sulphides—A review [J]. Hydrometallurgy, 2006, 84(1): 81−108.

[6] WANG Jun, ZHAO Hong-bo, ZHUANG Tian, QIN Wen-qing, ZHU

Shan, QIU Guan-zhou. Bioleaching of Pb−Zn−Sn chalcopyrite concentrate in tank bioreactor and microbial community succession analysis [J]. Transaction of Nonferrous Metals Society of China, 2013, 23(12): 3758−3762.
[7] OLSON G, BRIERLEY J, BRIERLEY C. Bioleaching review (part B) [J]. Applied Microbiology and Biotechnology, 2003, 63(3): 249−257.
[8] ZHAO H B, WANG J, HU M H, QIN W Q, ZHANG Y S, QIU G Z. Synergistic bioleaching of chalcopyrite and bornite in the presence of *Acidithiobacillus ferrooxidans* [J]. Bioresource Technology, 2012, 149: 71−76.
[9] ZHAO H B, WANG J, QIN W Q, HU M H, ZHU S, QIU G Z. Electrochemical dissolution process of chalcopyrite in the presence of mesophilic microorganisms [J]. Minerals Engineering, 2015, 71: 159−169.
[10] KLAUBER C. A critical review of the surface chemistry of acidic ferric sulphate dissolution of chalcopyrite with regards to hindered dissolution [J]. International Journal of Mineral Processing, 2008, 86(1): 1−17.
[11] GERICKE M, PINCHES A, van ROOYEN J. Bioleaching of a chalcopyrite concentrate using an extremely thermophilic culture [J]. International Journal of Mineral Processing, 2001, 62(1): 243−255.
[12] PRADHAN N, NATHSARMA K, SRINIVASA RAO K, SUKLA L, MISHRA B. Heap bioleaching of chalcopyrite: A review [J]. Minerals Engineering, 2008, 21(5): 355−365.
[13] GHAHREMANINEZHAD A, DIXON D, ASSELIN E. Electrochemical and XPS analysis of chalcopyrite ($CuFeS_2$) dissolution in sulfuric acid solution [J]. Electrochimica Acta, 2013, 87: 97−112.
[14] FARQUHAR M L, WINCOTT P L, WOGELIUS R A, VAUGHAN D J. Electrochemical oxidation of the chalcopyrite surface: An XPS and AFM study in solution at pH 4 [J]. Applied Surface Science, 2003, 218(1): 34−43.
[15] BIESINGER M C, LAU L W, GERSON A R, SMART R S C. Resolving surface chemical states in XPS analysis of first row transition metals, oxides and hydroxides: Sc, Ti, V, Cu and Zn [J]. Applied Surface Science, 2010, 257(3): 887−898.
[16] THIRD K, CORD-RUWISCH R, WATLING H. Control of the redox potential by oxygen limitation improves bacterial leaching of chalcopyrite [J]. Biotechnology and Bioengineering, 2002, 78(4): 433−441.
[17] HIROYOSHI N, KITAGAWA H, TSUNEKAWA M. Effect of solution composition on the optimum redox potential for chalcopyrite leaching in sulfuric acid solutions [J]. Hydrometallurgy, 2008, 91(1): 144−149.
[18] GERICKE M, GOVENDER Y, PINCHES A. Tank bioleaching of low-grade chalcopyrite concentrates using redox control [J]. Hydrometallurgy, 2010, 104(3): 414−419.
[19] ZHAO H B, WANG J, YANG C R, HU M H, GAN X, TAO L, QIN W Q, QIU G Z. Effect of redox potential on bioleaching of chalcopyrite by moderately thermophilic bacteria: An emphasis on solution compositions [J]. Hydrometallurgy, 2015, 151(0): 141−150.
[20] NAKAI I, SUGITANI Y, NAGASHIMA K, NIWA Y. X-ray photoelectron spectroscopic study of copper minerals [J]. Journal of Inorganic and Nuclear Chemistry, 1978, 40(5): 789−791.
[21] AVGOUROPOULOS G, IOANNIDES T. Selective CO oxidation over $CuO−CeO_2$ catalysts prepared via the urea–nitrate combustion method [J]. Applied Catalysis A: General, 2003, 244(1): 155−167.
[22] LIU W, FLYTZANI-STEPHANOPOULOS M. Transition metal-promoted oxidation catalysis by fluorite oxides: A study of CO oxidation over $CuCeO_2$ [J]. The Chemical Engineering Journal and the Biochemical Engineering Journal, 1996, 64(2): 283−294.
[23] LEFEVRE G, WALCARIUS A, EHRHARDT J J, BESSIERE J. Sorption of iodide on cuprite (Cu_2O) [J]. Langmuir, 2000, 16(10): 4519−4527.
[24] GHAHREMANINEZHAD A, ASSELIN E, DIXON D. Electrodeposition and growth mechanism of copper sulfide nanowires [J]. The Journal of Physical Chemistry C, 2011, 115(19): 9320−9334.
[25] CORDOBA E M, MUNOZ J A, BLAZQUEZ M L, GONZALE Z F, BALLESTER A. Leaching of chalcopyrite with ferric ion (Part II): Effect of redox potential [J]. Hydrometallurgy, 2008, 93(3): 88−96.
[26] YIN Q, KELSALL G, VAUGHAN D, ENGLAND K. Atmospheric and electrochemical oxidation of the surface of chalcopyrite ($CuFeS_2$) [J]. Geochimica et Cosmochimica Acta, 1995, 59(6): 1091−1100.
[27] MAJUSTE D, CIMINELLI V, OSSEO-ASARE K, DANTAS M, MAGALH ES-PANIAGO R. Electrochemical dissolution of chalcopyrite: Detection of bornite by synchrotron small angle X-ray diffraction and its correlation with the hindered dissolution process [J]. Hydrometallurgy, 2012, 111: 114−123.
[28] ZHAO Hong-bo, HU Ming-hao, LI Yi-ni, ZHU Shan, QIN Wen-qin, QIU Guan-zhou, WANG Jun. Comparison of electrochemical dissolution of chalcopyrite and bornite in acid culture medium [J]. Transactions of Nonferrous Metals Society of China, 2015, 25(1): 303−313.
[29] HARMER S L, THOMAS J E, FORNASIERO D, GERSON A R. The evolution of surface layers formed during chalcopyrite leaching [J]. Geochimica et Cosmochimica Acta, 2006, 70(17): 4392−4402.
[30] ACRES R G, HARMER S L, BEATTIE D A. Synchrotron XPS, NEXAFS, and ToF-SIMS studies of solution exposed chalcopyrite and heterogeneous chalcopyrite with pyrite [J]. Minerals Engineering, 2010, 23(11): 928−936.
[31] ACRES R G, HARMER S L, SHUI H W, CHEN C H, BEATTIE D A. Synchrotron scanning photoemission microscopy of homogeneous and heterogeneous metal sulfide minerals [J]. Journal of Synchrotron Radiation, 2011, 18(4): 649−657.
[32] DESCOSTES M, MERCIER F, THROMAT N, BEAUCAIRE C, GAUTIER-SOYER M. Use of XPS in the determination of chemical environment and oxidation state of iron and sulfur samples: Constitution of a data basis in binding energies for Fe and S reference compounds and applications to the evidence of surface species of an oxidized pyrite in a carbonate medium [J]. Applied Surface Science, 2000, 165(4): 288−302.

中度嗜热菌浸出黄铜矿过程表面产物解析

赵红波[1,2]，王 军[1,2]，覃文庆[1,2]，郑细华[1,2]，陶 浪[1,2]，甘晓文[1,2]，邱冠周[1,2]

1. 中南大学 资源加工与生物工程学院，长沙 410083；2. 中南大学 生物冶金教育部重点实验室，长沙 410083

摘 要：采用 X 射线衍射(XRD)与 X 射线光电子能谱(XPS)研究黄铜矿在中度嗜热菌浸出过程中的表面产物变化。结果表明，在 *A. caldus*, *S. thermosulfidooxidans* 与 *L. ferriphilum* 浸出过程中，一硫化物(CuS)、二硫化物(S_2^{2-})、元素硫(S^0)、多硫化物(S_n^{2-})与硫酸盐(SO_4^{2-})是黄铜矿表面的主要产物。在 *A. caldus* 浸出黄铜矿过程速率较慢，这主要是由于黄铜矿的不完全溶解产生多硫化物，限制了进一步的溶解。在 *S. thermosulfidooxidans* 与 *L. ferriphilum* 浸出黄铜矿过程中，多硫化物与黄钾铁矾是钝化膜的主要成分。元素硫不是导致黄铜矿生物冶金过程钝化的主要物质。

关键词：黄铜矿；表面产物；生物浸出；钝化；中度嗜热微生物

(Edited by Xiang-qun LI)